Ultra-broadband and high-efficiency polarization conversion metasurface with multiple plasmon resonance modes*

Guo-Xiang Dong(董果香)[1,2], Hong-Yu Shi(施宏宇)[2], Song Xia(夏颂)[1,2,†], Wei Li(李玮)[1,2], An-Xue Zhang(张安学)[1], Zhuo Xu(徐卓)[1,2], and Xiao-Yong Wei(魏晓勇)[1,2]

[1] *Electronic Materials Research Laboratory, Key Laboratory of the Ministry of Education & International Center for Dielectric Research, Xi'an Jiaotong University, Xi'an* 710049, *China*

[2] *School of Electronic and Information Engineering, Xi'an Jiaotong University, Xi'an* 710049 *China*

(Received 4 January 2016; revised manuscript received 31 March 2016; published online 25 June 2016)

In this paper, we present a novel metasurface design that achieves a high-efficiency ultra-broadband cross polarization conversion. The metasurface is composed of an array of unit resonators, each of which combines an H-shaped structure and two rectangular metallic patches. Different plasmon resonance modes are excited in unit resonators and allow the polarization states to be manipulated. The bandwidth of the cross polarization converter is 82% of the central frequency, covering the range from 15.7 GHz to 37.5 GHz. The conversion efficiency of the innovative new design is higher than 90%. At 14.43 GHz and 40.95 GHz, the linearly polarized incident wave is converted into a circularly polarized wave.

Keywords: polarization, metasurface, plasmon, ultra-broadband

PACS: 42.25.Bs, 42.25.Ja, 78.67.Pt, 92.60.Ta **DOI:** 10.1088/1674-1056/25/8/084202

1. Introduction

The polarization state is an important basic property of THE electromagnetic wave and researchers have made great efforts to manipulate it.[1,2] In recent years, metamaterials,[3,4] which have numerous intriguing artificial electromagnetic responses, have been proposed to control the polarization state. Some examples include birefringent metamaterial,[5–7] anisotropic metamaterials,[8–10] and chiral metamaterials.[11,12] Anisotropic or birefringent metamaterials have been designed to achieve cross polarization conversion and circular polarization, while chiral metamaterials have been proposed to realize cross polarization conversion and asymmetric transmission. Metasurfaces, which are essentially two-dimensional (2D) metamaterials,[13–15] can be used to control the polarization state in subwavelength range. Therefore, miniaturized polarization converters can be achieved by using metasurfaces. The polarization conversion working in terahertz and visible wavelength range has been widely examined. For instance, a bilayer plasmonic transmission-type metasurface operating at visible frequencies experimentally yields a conversion efficiency of 17% for anomalous refraction.[16] A compact broadband circular polarization analyzer in the meso-field has demonstrated that the light of different handedness is focused into a subwavelength confined spot or a ring-shaped intensity profile.[17] An ultrathin, terahertz quarter-wave plate based on planar babinet-inverted metasurface can convert linear polarization into circular polarization.[18] A concept of degenerated image dipole array is reported to realize anomalous light bending with high efficiency in nearly the entire visible band.[19] However, the narrow bandwidth of operation has restricted the practical applications of these polarization converters in microwave band. In general, the bandwidth can be broadened by using different techniques including stacking multilayer structures,[20] multiple plasmon resonances,[21] and plasmon hybridizations.[22] For instance, the double-head arrow metasurface[23] expands bandwidth of polarization conversion, but the conversion efficiency is just 50% within 3-dB bandwidth. The average conversion efficiency of anchor-shaped metasurface[24] is 80% within 3-dB bandwidth. The plasmon hybridization in C2-symmetric ring/disk cavity can be used to expand the bandwidth of the polarization converter, but the conversion efficiency is not very high. However, comparing with that of reflection-type metasurface, the cross-polarization conversion efficiency of the transmission-type metasurface[25] is fundamentally limited to below 25%. Therefore, the conversion efficiency and bandwidth of polarization conversion still need to be improved simultaneously to realize a practically useful device.

In this work, we propose a metasurface design to achieve ultra-broadband and high-efficiency polarization conversion simultaneously. The metasurface is composed of an array of unit cell resonators, each of which combines an H-shaped

*Project supported by the National Natural Science Foundation of China (Grant Nos. 61471292, 61331005, 61471388, 51277012, 41404095, and 61501365), the 111 Project, China (Grant No. B14040), the National Basic Research Program of China (Grant No. 2015CB654602), and the China Postdoctoral Science Foundation (Grant No. 2015M580849).

†Corresponding author. E-mail: sxia@mail.xjtu.edu.cn

© 2016 Chinese Physical Society and IOP Publishing Ltd

structure and two rectangular metallic patches. Three plasmon resonance modes are excited in the unit resonator, which modifies the phase distribution of the reflected waves, allowing the polarization states to be manipulated as desired. Simulations and experimental results show that the conversion efficiency is over 90% from 15.7 GHz to 37.5 GHz, which is 82% of the central frequency for both x and y polarized waves. Additionally, the proposed metasurface can also convert the linearly polarized wave into a circularly polarized wave. At 14.43 GHz and 40.95 GHz, the linearly incident wave is converted into a left handed or right handed circularly polarized wave respectively.

2. Metasurface design

The anisotropic metasurface has the potential to achieve cross polarization conversion. Furthermore, wideband polarization conversion can also be achieved by using multiple plasmon resonances. Individually cut wire resonators support multi-order dipolar resonances; an individual H-shaped structure and a rectangular metallic structure can be seen as cut wire resonators in a particular direction. Combining these two structures yields a metasurface that can support multiple plasmon resonances while giving the designer more controls over device characteristics. The unit cell structure of the proposed metasurface is shown in Fig. 1(a). It can be divided into two parts: one part consists of two rectangular metallic patches, and the other part consists of an H-shaped structure that lies between the metallic patches. As shown in Fig. 1(b), the structure of the proposed metasurface is symmetric across v axis, which is the axis along the 45° direction with respect to the y direction. Hence, the metasurface is an anisotropic structure. The geometrical parameters of the proposed metasurface are given by $p = 3.9$ mm, $l = 3.8$ mm, $g = 1.2$ mm, $d = 0.2$ mm, $w = 0.2$ mm, $a = 1.7$ mm, and $b = 1.1$ mm. The dielectric spacer parameters are permittivity $= 2.62$ and loss tangent tan $\delta = 0.001$. The thickness of the substrate is 1.45 mm, and a metallic sheet is placed on the back side of the substrate to ensure that almost all of the incident power is reflected.

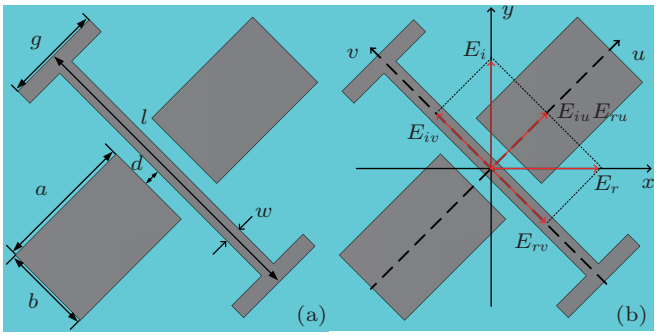


Fig. 1. (color online) (a) Proposed structure of the metasurface. (b) Intuitive image of y-polarized incident wave rotated to x-polarized reflection wave.

3. Results and theoretical analysis

3.1. Simulation results

The frequency domain solver in CST Microwave Studio is used to numerically investigate the ultra-broadband property of the proposed metasurface. The cross-polarization reflectances are defined as $r_{xy} = E_{xr}/E_{yi}$, $r_{yx} = E_{yr}/E_{xi}$, and co-polarization reflectances are defined as $r_{yy} = E_{yr}/E_{yi}$, $r_{xx} = E_{xr}/E_{xi}$. The subscripts r and i denote the reflected wave and the incident wave respectively; the subscripts y and x refer to the two polarization directions of the wave. The polarization conversion ratio (PCR) is defined as PCR $= r_{xy}^2/(r_{xy}^2 + r_{yy}^2)$. The stimulated results are plotted in Fig. 2. Figure 2(a) shows the co-polarization and cross-polarization ratios versus frequency. Figure 2(b) shows a plot of PCR versus frequency. The bandwidth of the cross-polarization conversion is 21.8 GHz (from 15.7 GHz to 37.5 GHz), which is 82% of the central frequency, and the polarization conversion ratio is higher than 90%. In Table 1, the proposed metasurface is compared with other polarization converters, which shows that the proposed metasurface achieves wide bandwidth and efficient polarization conversion, simultaneously.

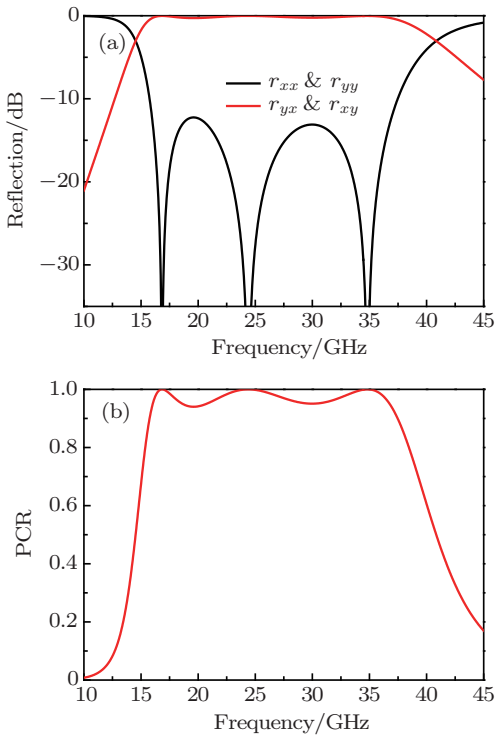


Fig. 2. (color online) Simulated results of (a) co- and cross-polarization reflections and (b) the polarization conversion ratio.

Table 1. Comparison of the proposed metasurface with other reflection-type polarization conversion metasurfaces.

	Frequency band/GHz	Central bandwidth	Conversion efficiency
Ref. [23]	17.9	84%	50%
Ref. [22]	4.51	38%	80%
Ref. [24]	5	28.5%	90%
Our work	21.8	82%	90%

3.2. Cross polarization conversion mechanism

In order to understand the enhanced polarization conversion efficiency of the proposed metasurface, the plasmon resonances of the unit cell are studied. The reflectances for an incident wave polarized along the v axis and u axis are shown in Figs. 3(a) and 3(b) respectively. The results indicate that the reflectance is higher than -0.06 dB (0.993) in a range from 15.7 GHz to 37.5 GHz. It is also shown that there are a total of three reflectance dips, which indicates that three plasmon resonances are excited in the unit structure of the metasurface as shown in Fig. 3.

To be able to intuitively understand the plasmon resonances,[16] the simulated distributions of the electric field of the proposed metasurface at plasmon resonances are shown in Fig. 4. For the incident wave polarized along the v axis, two plasmon resonances are excited as shown in Fig. 3(a). At plasmon resonance (i), the rectangular metallic patches are excited in their dipolar mode along the v axis. As shown in Fig. 4(a), this mode is in phase with the dipolar mode of the middle H-shape structure. At plasmon resonance (iii), the rectangular metallic patches are excited in dipolar mode along the v axis. As shown in Fig. 4(c), this mode is out of phase with the dipolar mode of the middle H-shape structure.

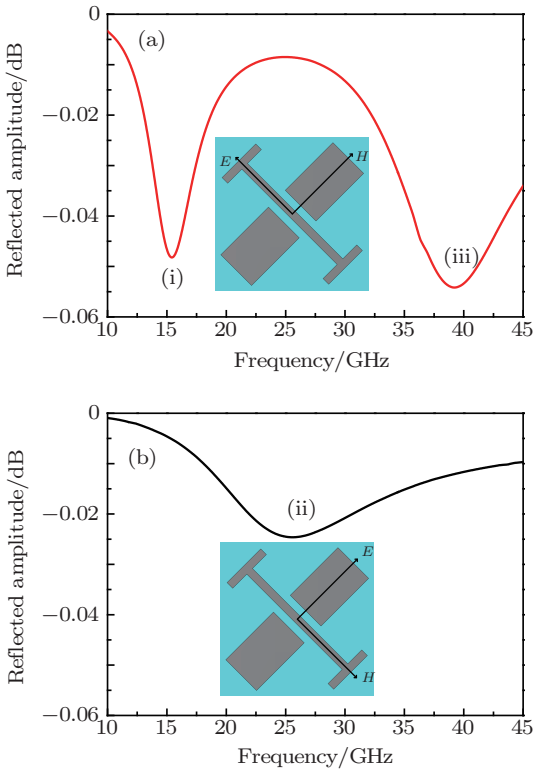


Fig. 3. (color online) Frequency-dependent reflected amplitudes for an incident wave polarized along (a) the v axis and (b) the u axis of the metasurface.

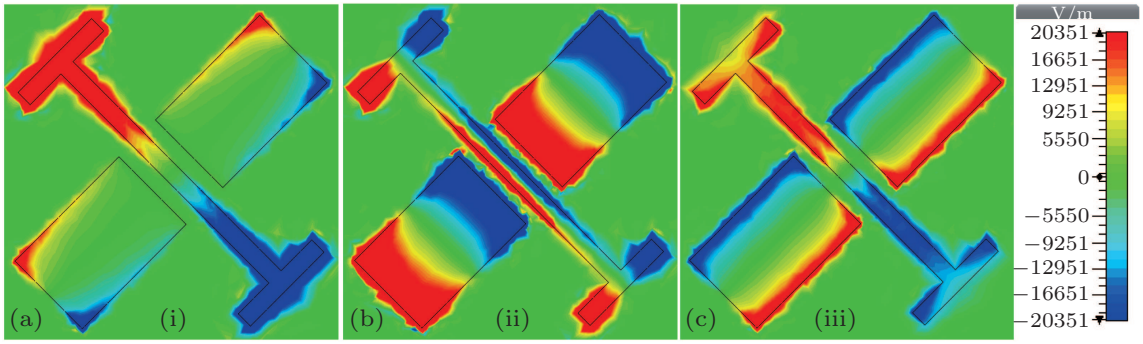


Fig. 4. (color online) Simulated distributions of the electric field E_z of the metasurface unit cell at (a) plasmon resonances (i), (b) plasmon resonances (ii), (c) plasmon resonances (iii).

For the incident wave polarized along the u axis, there is only one plasmon resonance as shown in Fig. 3(b). The rectangular metallic patches are excited in dipolar mode along the u axis as shown in Fig. 4(d); this is in phase with the dipolar mode of the middle H-shape structure. Moreover, the three plasmon resonances have different resonance modes from each other as shown in Fig. 4.

To understand how multiple plasmon resonances contribute to the ultra-broadband polarization conversion, the phases of the reflected signal for incident waves polarized along the v axis and u axis are shown in Fig. 5. As shown in Fig. 3, there are two plasmon resonances when the incident wave is polarized along the v axis, and one plasmon resonance when it is polarized along the u axis. The combination of these resonances causes the phase difference between the reflected wave along the u axis and v axis to be 180° from 15.7 GHz to 37.5 GHz as shown in Fig. 5. If the incident wave is polarized along the y axis, it can be decomposed into individual components that are polarized along both the v and the u axes. Because of the 180° phase difference between the reflected wave along the v axis and the reflected wave along the u axis, the total reflected wave would be polarized along the x axis. Hence, an ultra-broadband cross polarization conversion will be achieved. Notably, at 14.43 GHz and 40.95 GHz, the phase differences between the reflected wave along the v axis and the reflected wave along the u axis are $-90°$ and 90° respectively. Thus, the total reflected waves would be circularly polarized at 14.43 GHz and 40.95 GHz respectively.

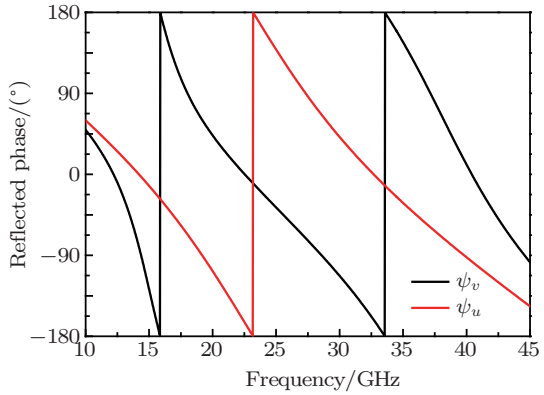


Fig. 5. (color online) Reflected phases for an incident wave polarized along the *v* axis and the *u* axis of the metasurface.

4. Results and theoretical analysis

A 410 mm×410 mm sample of the metasurface as shown in Fig. 6(a), is fabricated to further verify the design through actual measurements. The measurement setup is shown in Fig. 6(b). In this setup, two horn antennas are used: one is to radiate electromagnetic (EM) waves onto the sample, and the other is to receive the reflected waves from the sample. The two horn antennas are kept at the same vertical distance from the center of the sample to ensure that the wave can be reflected off the sample and received by the receiving antenna. The two horn antennas support TM and TE modes on different sides. When the radiating horn antenna is fixed, the receiving horn antenna can be placed on its longer and shorter sides, to measure the cross- and co-polarization conversion respectively. The measured cross- and co-polarization conversion results along with the simulation results are plotted in Fig. 6(c). The measured results are in agreement with the simulation results, verifying the concept behind the proposed metasurface. The measured bandwidth of the cross-polarization conversion is 21.4 GHz, which matches very closely with the 21.8 GHz predicted through simulations. There is a small difference between the measured and simulated results. In our simulations, the unit cell boundary conditions in CST Microwave Studio are set on the four lateral boundaries and open add space boundaries are set to be along the incidence direction. Hence, the metasurface is assumed to be infinite and the port covers the total metasurface. Thus, the incidence wave can be totally reflected with 180° phase difference along the *u* axis and *v* axis, meaning that the reflective wave will have a higher reflection in cross-polarization and smaller reflection in co-polarization. However, in the actual experiment, the metasurface is finite, which cannot guarantee the 180° phase difference in the entire reflective wave, especially when the wave is reflected from the edge of the metasurface. Therefore, the measured cross-polarization reflection is not so high as that shown in the simulation results, and the measured co-polarization reflection is not so small as in that indicated in the simulation results either. Furthermore, the error from its fabrication may also cause the difference between the measured and simulated results. The measured PCR indicate that the metasurface has a high-polarization conversion efficiency, which matches well with the simulated PCR as shown in Fig. 6(d).

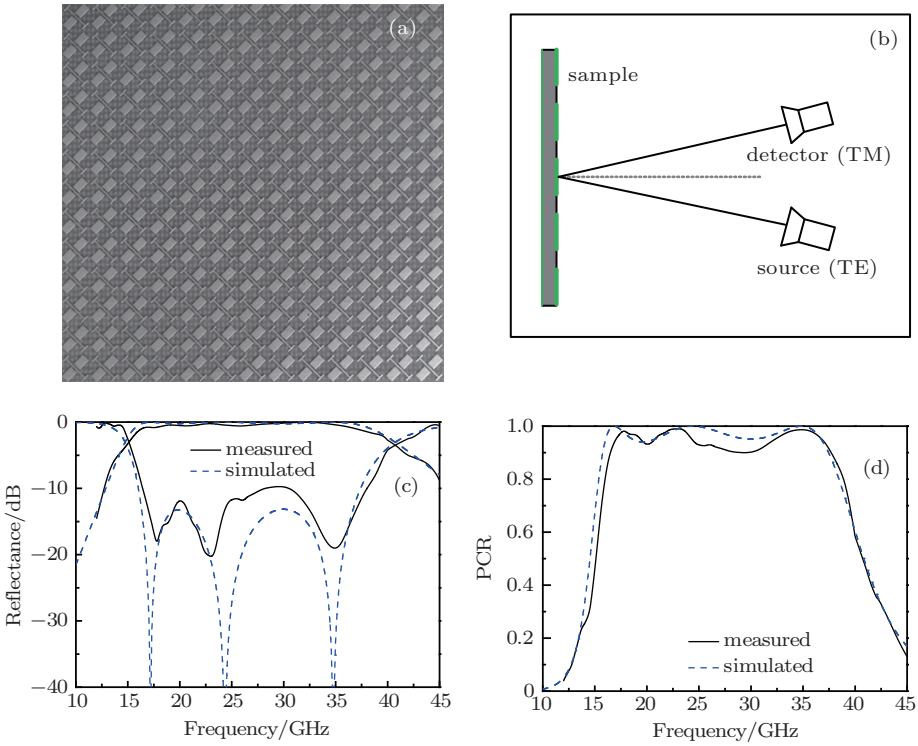


Fig. 6. (color online) (a) A fabricated sample of the metasurface, (b) schematic plot of measurement setup, (c) the simulated and the measured cross- and co-polarization reflections, and (d) the simulated, and the measured PCR.

5. Conclusions

In this work, we demonstrate an ultra-broadband and high-efficiency polarization converter by using an innovative metasurface design. By combining structures in the unit cell resonator to cause different plasmon resonance modes, the phase difference of the reflected wave along the v axis and the u axis is designed to be nearly 180° over a wide bandwidth. This leads to cross-polarization conversion from 15.7 GHz to 37.5 GHz with a conversion efficiency of over 90%, and a bandwidth that is 82% of the central wavelength for both x and y polarized waves. At 14.43 GHz and 40.95 GHz, the phase differences between the reflected waves along the v axis and the reflected waves along the u axis are $-90°$ and 90° respectively. Thus, the $x(y)$-polarized incident wave is converted into a left (right)-handed and a right (left)-handed circularly polarized wave respectively.

References

[1] Aieta F, Genevet P, Yu N F, Kats M A, Gaburro Z and Capasso F 2012 *Nano Lett.* **12** 1702
[2] Pfeiffer C and Grbic A 2013 *Appl. Phys. Lett.* **102** 231116
[3] Wu Q N, Lan F, Tang X P and Yang Z Q 2015 *Chin. Phys. Lett.* **32** 107801
[4] Shi J X, Zhang W C, Xu W, Zhu Q, Jiang X, Li D D, Yan C C and Zhang D H 2015 *Chin. Phys. Lett.* **32** 094204
[5] Farmahini-Farahani M and Mosallaei H 2013 *Opt. Lett.* **38** 462
[6] Ma H F, Wang G Z, Kong G S and Cui T J 2014 *Opt. Mater. Express* **4** 1717
[7] Liu Y, Ling X, Yi X, Zhou X, Luo H and Wen S 2014 *Appl. Phys. Lett.* **104** 191110
[8] Chin J Y, Lu M and Cui T J 2008 *Appl. Phys. Lett.* **93** 251903
[9] Mingbo P, Po C and Yanqin W 2013 *Appl. Phys. Lett.* **102** 131906
[10] Yang Z and Alu A 2011 *Phys. Rev. B* **84** 205428
[11] Shi J H, Ma H F, Guan C Y, Wang Z P and Cui T J. 2014 *Phys. Rev. B* **89** 165128
[12] Jinhui S, Xingchen L and Shengwu Y 2013 *Appl. Phys. Lett.* **102** 191905
[13] Ye Y and He S 2010 *Appl. Phys. Lett.* **96** 203501
[14] Mutlu M and Ozbay E. A 2012 *Appl. Phys. Lett.* **100** 051909
[15] Hao J, Yuan Y and Ran L 2007 *Phy. Rev. Lett.* **99** 063908
[16] Qin F, Ding L, Zhang L, Monticone F, Chum C C, Deng J, Mei S, Li Y, Teng J, Hong M, Zhang S and Alo A 2016 *Sci. Adv.* **2** e1501168
[17] Mehmood M Q, Liu H, Huang K, Mei S, Danner A, Luk'yanchuk B, Zhang S, Teng J, Maier S A and Qiu C W 2015 *Laser Photon. Rev.* **9** 674
[18] Wang D, Gu Y, Gong Y, Qiu C W and Hong M 2015 *Opt. Express* **23** 11114
[19] Zhang L, Hao J, Qiu M, Zouhdi S, Yang J K W and Qiu C W 2014 *Nanoscale* **61** 2303
[20] Wei Z, Cao Y, Fan Y, Yu X and Li H 2011 *Appl. Phys. Lett.* **99** 221907
[21] Feng M, Wang J, Ma H, Mo W, Ye H and Qu S 2013 *J. Appl. Phys.* **114** 074508
[22] Shi H, Li J, Zhang A, Wang J and Xu Z 2014 *Opt. Express* **22** 20973
[23] Chen H, Wang J and Ma H 2014 *J. Appl. Phys.* **115** 154504
[24] Yin J Y, Wan X, Zhang Q and Cui T J 2015 *Sci. Rep.* **5** 12476
[25] Ding X, Monticone F, Zhang K, Zhang L, Gao D, Burokur S N, de Lustrac A, Wu Q, Qiu C W and Alu A 2015 *Adv. Mater.* **27** 1195